

# Glaciation as a destructive and constructive control on mountain building

Stuart N. Thomson<sup>1,2</sup>, Mark T. Brandon<sup>2</sup>, Jonathan H. Tomkin<sup>4</sup>, Peter W. Reiners<sup>1</sup>, Cristián Vásquez<sup>3</sup> & Nathaniel J. Wilson<sup>2</sup>

Theoretical analysis predicts that enhanced erosion related to late Cenozoic global cooling can act as a first-order influence on the internal dynamics of mountain building, leading to a reduction in orogen width and height<sup>1–3</sup>. The strongest response is predicted in orogens dominated by highly efficient alpine glacial erosion, producing a characteristic pattern of enhanced erosion on the windward flank of the orogen and maximum elevation controlled by glacier equilibrium line altitude<sup>3,4</sup>, where long-term glacier mass gain equals mass loss. However, acquiring definitive field evidence of an active tectonic response to global climate cooling has been elusive<sup>5</sup>. Here we present an extensive new low-temperature thermochronologic data set from the Patagonian Andes, a high-latitude active orogen with a well-documented late Cenozoic tectonic, climatic and glacial history. Data from 38° S to 49° S record a marked acceleration in erosion 7 to 5 Myr ago coeval with the onset of major Patagonian glaciation<sup>6</sup> and retreat of deformation from the easternmost thrust front<sup>7</sup>. The highest rates and magnitudes of erosion are restricted to the glacial equilibrium line altitude on the windward western flank of the orogen, as predicted in models of glaciated critical taper orogens where erosion rate is a function of ice sliding velocity<sup>3,8</sup>. In contrast, towards higher latitudes (49° S to 56° S) a transition to older bedrock cooling ages signifies much reduced late Cenozoic erosion despite dominantly glacial conditions here since the latest Miocene<sup>6</sup>. The increased height of the orogenic divide at these latitudes (well above the equilibrium line altitude) leads us to conclude that the southernmost Patagonian Andes represent the first recognized example of regional glacial protection of an active orogen from erosion, leading to constructive growth in orogen height and width.

The excellent match between non-volcanic summit elevations and southward decrease in perennial snowline in the southern Andes is cited as a classic example of first-order climatic control on mountain topography<sup>9–11</sup>. According to the glacial ‘buzzsaw’ hypothesis, highly efficient alpine glacial erosion limits the development of topography above the glacial equilibrium line altitude (ELA)<sup>13</sup>. Supporting this hypothesis, in the northern Patagonian Andes the match between elevation and snowline is maintained despite widely variable late Cenozoic rock uplift rates<sup>12</sup>. However, south of about 45° S, this relationship breaks down<sup>14</sup>, with the summits and mean elevation of the orogenic divide situated well above the long-term mean ELA, in conflict with the idea of a global glacial buzzsaw<sup>11,13</sup>.

A strong link between glaciation and reduction in topographic relief is a key component of recent models that demonstrate that enhanced erosion associated with late Cenozoic climate change can alter the internal dynamics of active mountain belts<sup>1,3,15</sup>. These models call into question earlier claims that climatically enhanced late Cenozoic erosion rates and isostatic rebound increased relief and summit

elevations, inducing a positive feedback of more erosion and rock uplift, and the illusion of increased tectonic activity<sup>16</sup>. Demonstrating the validity of these model-based arguments using field observations is complicated by complex real-world interactions between climate change, erosion and tectonics<sup>5</sup>. Increased rock uplift, erosion, and sediment supply in response to climate change alone is insufficient to distinguish between an active tectonic or passive isostatic response to climate change. True diagnosis requires that such increases are accompanied by a reduction in the height and width of a critical-taper orogen, with deformation retreating to the core of the range<sup>5</sup>.

We chose to test these concepts by applying low-temperature thermochronometry to evaluate spatial and temporal patterns of erosion in the glaciated Patagonian Andes, including higher latitudes where the match between elevation and snowline breaks down. Glaciated orogens are theoretically more responsive to changes in climate and tectonics than fluvially dominated orogens<sup>3</sup>, making any response more readily detectable. Widespread mountain glaciation in Patagonia began sometime between 7 and 5 Myr ago (ref. 6), providing a much longer record than comparable Northern Hemisphere orogens<sup>4</sup>. This time span is similar to typical predicted response times of glaciated orogens to changes in climate and tectonics of 1.5 to 5.5 Myr (ref. 3).

We report 246 new apatite (U–Th)/He ages and 136 new apatite fission-track (AFT) ages from 146 samples collected along the length and breadth of the Patagonian Andes from 38° S to 56° S, as well as 165 previously published AFT ages (Fig. 1, Supplementary Note 2 and Supplementary Tables 1–3). All ages less than about 10 Myr that are relevant to our interpretations are considerably younger than the stratigraphic or magmatic crystallization age of the rocks and reflect the time of cooling related to removal of overburden by erosion.

Apatite (U–Th)/He and AFT age–elevation relationships from close to the main divide in the more northerly parts of the Patagonian Andes (Fig. 2) demonstrate a marked change from older (high elevation) to younger (low elevation) ages, indicative of an acceleration of erosion rates<sup>17</sup> at about 7 Myr ago. The timing of this acceleration is well after the onset of initial surface uplift of the Patagonian Andes, dated to around 17–14 Myr ago<sup>18</sup>, but is remarkably similar to the onset of widespread glaciation in the region<sup>6</sup>, supporting the previously recognized strong erosional response of the orogen at these latitudes to cooler climate and the onset of erosive alpine glaciation<sup>12</sup>. More importantly, a diagnostic active tectonic response to climatic cooling is implied by contemporaneous cessation of faulting at the easternmost thrust front at similar latitudes between 9 and 6 Myr ago<sup>7,12</sup>, with shortening confined to more internal parts of the orogen, recorded locally by a transition from strike-slip motion to transpressional uplift along the Liquiñe–Ofqui fault since ~7 Myr ago<sup>12</sup>.

<sup>1</sup>Department of Geosciences, University of Arizona, Tucson, Arizona 85721, USA. <sup>2</sup>Department of Geology and Geophysics, Yale University, New Haven, Connecticut 06511, USA. <sup>3</sup>Departamento de Geología, Universidad de Chile, Casilla 13518, Correo 21, Santiago, Chile. <sup>4</sup>Department of Geology, University of Illinois, Urbana, Illinois 61801, USA.

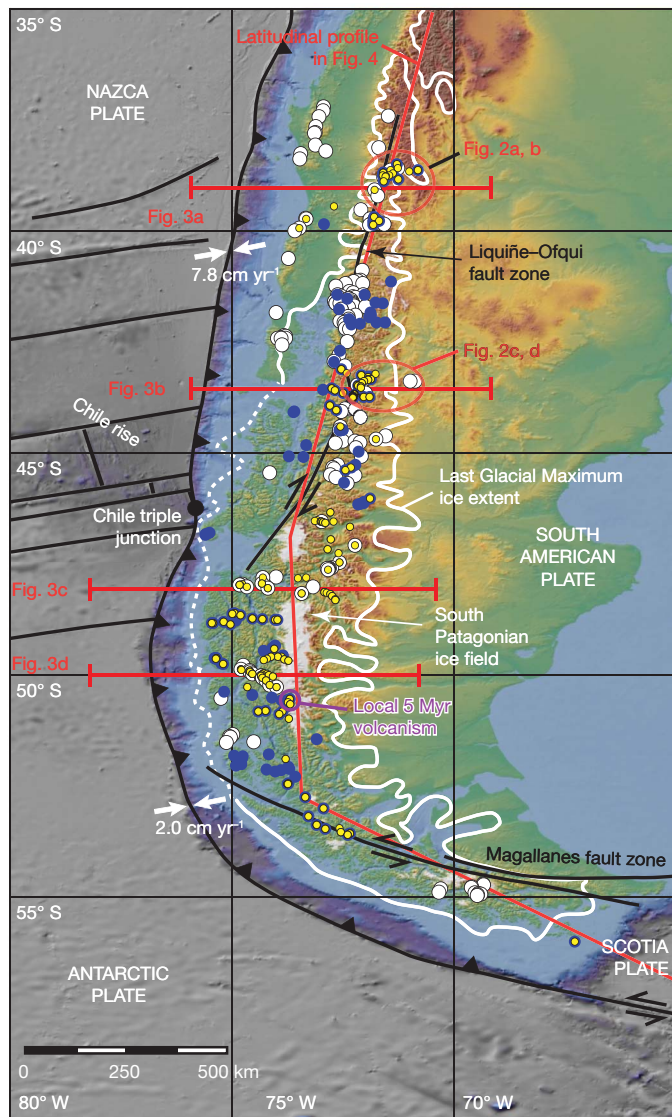


**Figure 1 | Topographic and tectonic map of southernmost South America showing sample locations.** Apatite (U–Th)/He locations are shown as small yellow circles; AFT locations are shown as medium blue circles. Also included are the locations of samples used to plot age–elevation relationships in Fig. 2, the positions of the transects shown in Fig. 3, and the latitudinal profile in Fig. 4 (all marked in red). Details on previously published apatite fission-track samples (large white circles), digital elevation data, location of Last Glacial Maximum ice extent (delimited by white line), volcanic ages (purple circle), and plate convergence velocities (white arrow pairs) are given in Supplementary Notes 1 and 2, and Supplementary Table 3.

The spatial patterns of both AFT and apatite (U–Th)/He ages across three transects north of 49° S (Fig. 3a–c) reveal a distinct U-shaped pattern, with the age minima (<5 Myr)—and hence the highest magnitude and rates of erosion—concentrated where the ELA intersects the topography on the windward western flank of the orogen. This pattern matches the predictions of numeric and analytic models of the expected erosional response to increased alpine glaciation in critical taper orogens<sup>3,8</sup>, and is a characteristic feature of the windward flank of other high-latitude orogens dominated by temperate alpine glaciation<sup>4,19</sup>. In such orogens an additional link between precipitation rate and thermochronometric age minima has been recognized<sup>19</sup>. A natural coupling between maximum erosion rates, precipitation rates, and the intersection of ELA with topography is to be expected, because enhanced precipitation in the form of snowfall on the windward flank results in thicker ice close to the ELA, with resultant increased sliding velocity and

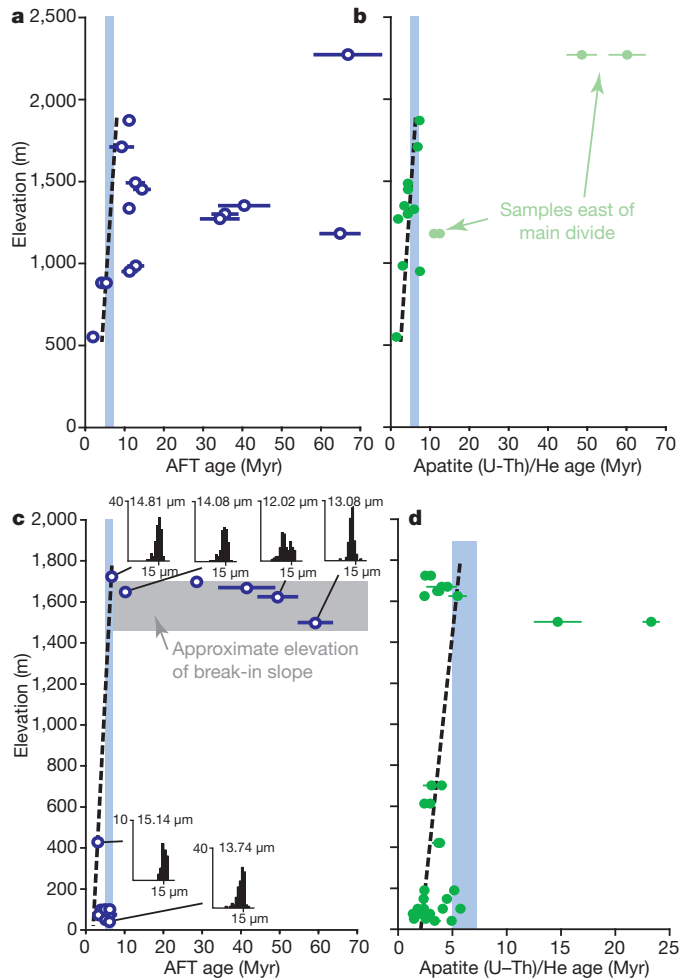


**Figure 2 | Age–elevation relationships from two high-relief transects.** The reference slope is 0.5 mm yr<sup>−1</sup> (black dashed line in all panels). The onset of glaciation is 5–7 Myr ago (thick blue line in all panels). **a**, AFT age–elevation relationship (AER) from 38–40° S. **b**, Apatite (U–Th)/He AER from the same samples, showing younger ages at lower elevations, indicative of the onset of enhanced erosion ~7 Myr ago coeval with the onset of major glaciation in southern South America. **c**, AFT AER from 43–44° S showing a similar transition to younger ages with longer mean-track-length distributions (histograms for the indicated data points show mean track length versus number of fission tracks) at lower elevations ~7 Myr ago. The break-in slope<sup>17</sup> approximates the former closure depth of the thermochronometric system (~4.1 km for AFT for erosion rates of ~0.5 mm yr<sup>−1</sup>; ref. 30) immediately before accelerated erosion ~7 Myr ago. This equates to a time-averaged erosion rate of ~0.6 mm yr<sup>−1</sup> since then. The samples close to sea level represent an additional 1.5 km of erosion (total of 5.6 km erosion) requiring a time-averaged erosion rate of 0.8 mm yr<sup>−1</sup> since 7 Myr ago. **d**, Apatite (U–Th)/He ages from the same samples show a similar AER. All age error bars that are larger than the symbol are 1 sigma.

basal shear stress leading to higher localized erosion rates. Further support for glacially enhanced erosion, rather than the location of local active structures, as a control on the observed age patterns across these three northernmost transects is provided by the presence of an age minimum close to the ELA on the windward flank in the absence of any arc-parallel faulting between 47–49° S (Fig. 3c). The observed correlation between timing of onset of glaciation, deformation front retreat, and concentration of deformation and acceleration of erosion rates within the orogen interior supports the idea of the Patagonian Andes north of ~47–49° S as being one of the most convincing examples worldwide of the destructive active tectonic response of an orogen (through its reduction in width and height) to climate change and the onset of glaciation.

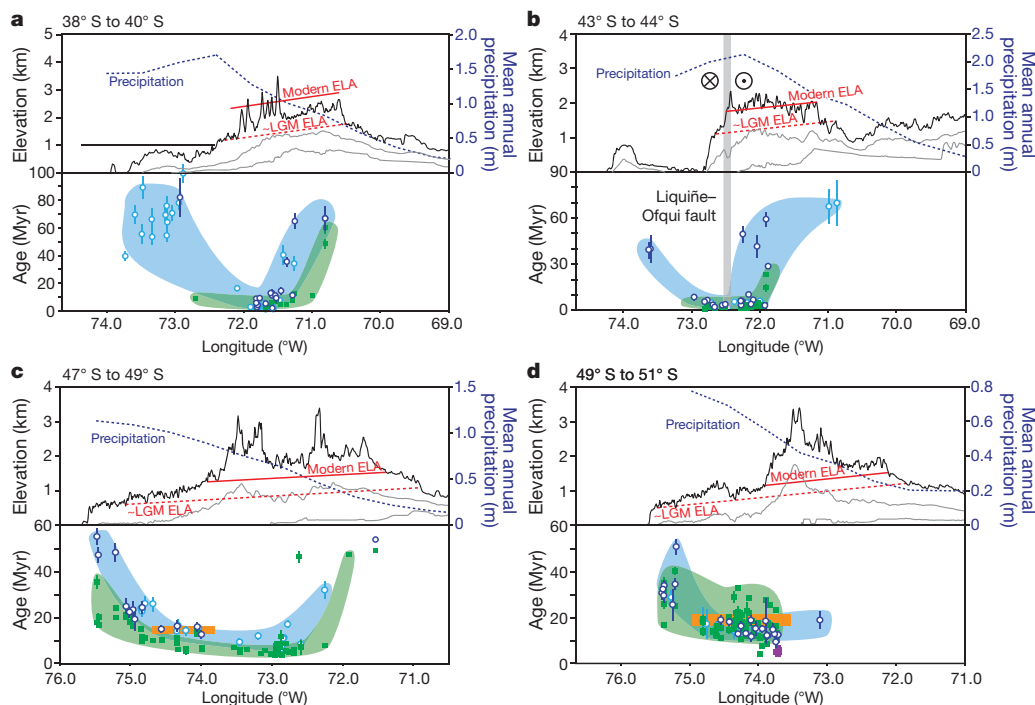


**Figure 3 | Four east-west transects across the Patagonian Andes at different latitudes.** New apatite (U–Th)/He ages are shown as green circles, new AFT ages as dark blue circles, and the previously published AFT ages as light blue circles; 1 sigma error bars. **a–c**, The three northernmost transects show a distinct U-shaped age minimum for both thermochronometers (less than about 5 Myr ago) on the windward (enhanced precipitation) side of the range whereas the profile furthest south (**d**) shows no such relationship,

In contrast, the more southerly transect at 49–51° S (Fig. 3d) shows exclusively old apatite (U–Th)/He and AFT ages >10 Myr (with the exception of several local ~5-Myr-old volcanic rocks), which implies inefficient regional glacial erosion at these latitudes over the last ~10 Myr. A southward increase in the youngest age (and hence a decrease in long-term glacial erosion efficiency) across the whole orogen can be seen clearly in latitudinal swath profiles (Fig. 4). For both systems this transition occurs between about 45° S and 50° S, being more apparent in the fission-track data. Importantly, this transition coincides in latitude with an increase in the non-volcanic maximum and mean elevation of the main divide south of ~45° S to well above the Last Glacial Maximum and the modern ELA, demonstrating that the southernmost Patagonian Andes do not support the glacial buzzsaw hypothesis<sup>11</sup>. A regional decrease in erosional efficiency at these latitudes is supported by a southward decrease in the amount of glacial-marine fjord sedimentation from thick temperate glacial facies north of 46° S, to thinner transitional polar glacial facies at ~54° S (ref. 20), as well as by the preservation of 5-Myr-old dacite lava flows forming islands in a fjord at 50° S (ref. 21).

The remarkable latitudinal coincidence between lower glacial erosion efficiency and higher elevations of the southern Patagonian Andes is consistent with glaciation having acted effectively at a regional orogenic scale to protect the landscape from erosion over much of the latest Cenozoic era. In critical-taper orogens, if there is no change in accretionary flux, a decrease in erosional efficiency (and hence reduced erosional efflux) is predicted to act in a constructive manner, leading to an increase in wedge width and height<sup>5,15</sup>. The assumption of no change in accretionary flux in the Patagonian Andes is corroborated by at least 10 Myr of steady subduction of the Antarctic plate south of ~48° S (ref. 7). Furthermore, if the approximately 1,000 m higher elevation of the divide at these latitudes were the result of surface uplift owing to the lack of significant erosion since the onset of widespread glaciation ~7 to 5 Myr ago, this would require time-averaged tectonic and surface uplift rates of ~0.14 to 0.2 mm yr<sup>-1</sup>. These rates match

despite the presence of widespread fjords and ongoing glaciation. Transects include age data, mean, maximum, and minimum elevation information from a 1° swath (**a**, **c**, **d**) or 0.5° swath (**b**) either side of each transect. The ELA is from refs 9 and 14. The mean annual precipitation data are from the UNEP/GRID database (<http://www.grid.unep.ch/>). The highlighted region of Miocene (about 20 Myr ago) magmatism (orange) places an upper age limit on most of the samples from this part of the transect.

remarkably well with post-early Miocene surface uplift rates of 0.07 to 0.22 mm yr<sup>-1</sup> estimated from 1,900 m elevation transitional marine facies rocks at 47° S (ref. 22). Evidence for increasing wedge width is implied by active reverse fault scarps and tilting of Pliocene basalts at the eastern mountain front at 49° 30' S (ref. 23), as well as by coeval (6 to 5 Myr ago) uplift and denudation<sup>24</sup> and late Cenozoic eastward-migrating deep-seated thrusts<sup>25</sup> on the eastern side of the orogen at 51° S.

The lack of regionally extensive erosion south of about 45° S implies that any glacier basal flow (and hence erosive potential) must have been very spatially restricted. This agrees with a coupled ice-sheet/climate numeric model of the Patagonian icesheet<sup>26</sup>, in which during the Last Glacial Maximum high ice-flow velocities are limited to relatively widely spaced, very narrow ice-streams at the margins of the ice sheet, surrounded by extensive areas of very-low-velocity ice. The predominance of highly resistant granitic bedrock and complex geologically controlled fjord geometry south of about 45° S probably further acted to confine regions of fast-flowing ice, as well as limit basal ice flow, as has been proposed to explain limited erosion in the tectonically inactive East Greenland fjord region<sup>27</sup> (see Supplementary Note 3 for additional discussion).

Previously, glacial preservation of landscape has only been documented beneath ice sheets and ice caps in tectonically passive polar continental settings<sup>28,29</sup>. Consequently, the southernmost Patagonian Andes represent the first demonstrable example of regional glacial protection of an active orogen resulting in a constructive tectonic response to late Cenozoic climate cooling. That glaciation can act to protect an active orogen from erosion opens up the intriguing possibility that, given favourable glacio-climatic, geologic and tectonic conditions, a cooling climate can act to enhance topographic relief, not in the manner originally envisaged in ref. 16 through passive isostatic response to locally enhanced erosion, but by inhibiting erosion to promote further accretionary growth in orogen height and width.

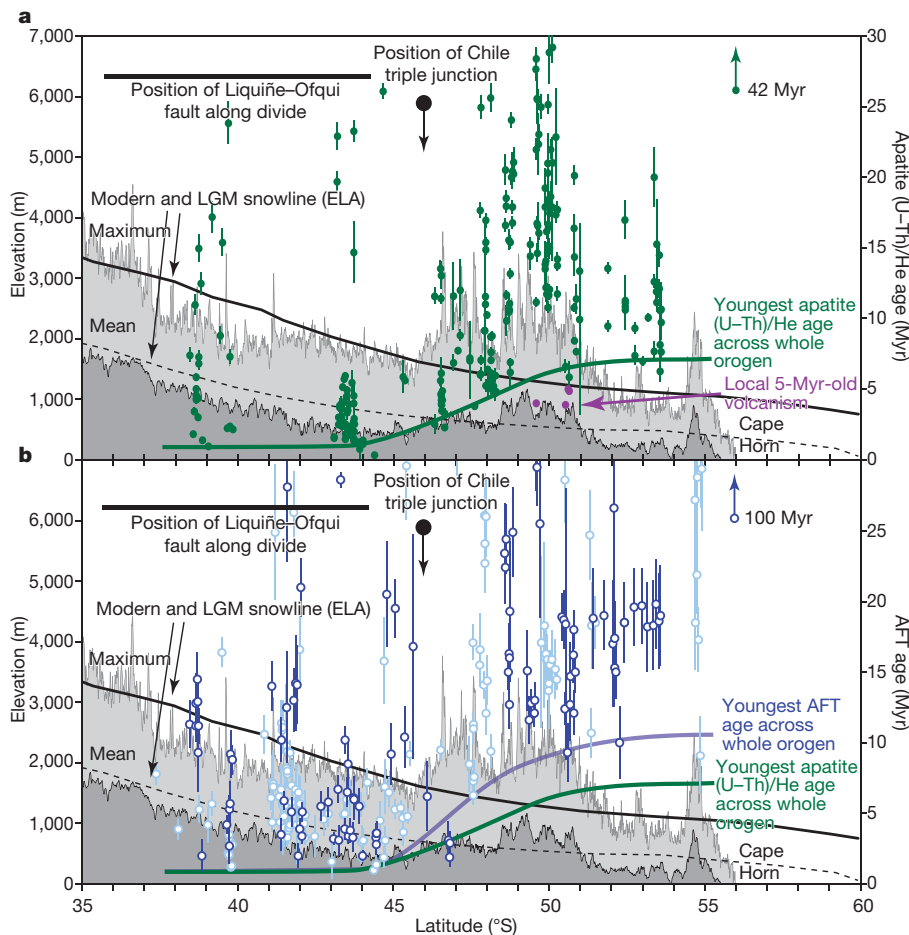


**Figure 4 | Latitudinal swath profiles showing apatite (U-Th)/He and AFT ages.** Also plotted are maximum and mean elevation (from a 4° east-west swath centred along the profile in Fig. 1), as well as the modern and mean glacial ELA<sup>14</sup>. **a**, Apatite (U-Th)/He ages (green circles); **b**, AFT ages (new AFT ages are shown as dark blue circles and the previously published AFT ages as light blue circles). All age error bars are 1 sigma. We note that with the

exception of some ages from independently dated Pliocene (5-Myr-old) dacite at about 50° S (ref. 21), the minimum apatite (U-Th)/He and AFT ages both show a distinct increase south of about 45° S, implying a significant decrease in total amounts and rates of post-10-Myr-ago erosion at these latitudes, despite dominantly glacial conditions here since ~7 Myr ago.

## METHODS SUMMARY

(U-Th)/He dating was performed on handpicked apatite grains measured for alpha-ejection correction following methods in ref. 19. Single or multiple crystals were loaded into 1 mm Pt tubes, and degassed by heating with a Nd-YAG laser. The concentration of <sup>4</sup>He was determined by <sup>3</sup>He isotope dilution and a quadrupole mass spectrometer. U, Th and Sm concentrations were obtained by isotope dilution using an inductively coupled plasma mass spectrometer. Alpha-ejection correction was applied to derive a corrected (U-Th)/He age. Fission track dating was done following the methods in ref. 12. CN5 and IRMM540R glass was used to monitor neutron fluence during irradiation at the Oregon State University Triga Reactor, Corvallis, USA. Zeta calibration factors of  $342.5 \pm 3.8$  (CN5 apatite), and  $352.4 \pm 12.1$  (IRMM540R apatite) were used in the calculation of central ages.

Received 9 March; accepted 15 July 2010.

- Whipple, K. X. & Meade, B. J. Orogen response to changes in climatic and tectonic forcing. *Earth Planet. Sci. Lett.* **243**, 218–228 (2006).
- Stolar, D., Roe, G. & Willett, S. Controls on the patterns of topography and erosion rate in a critical orogen. *J. Geophys. Res.* **112**, F04002, doi:10.1029/2006JF000713 (2007).
- Tomkin, J. H. & Roe, G. H. Climate and tectonic controls on glaciated critical-taper orogens. *Earth Planet. Sci. Lett.* **262**, 385–397 (2007).
- Berger, A. L. *et al.* Quaternary tectonic response to intensified glacial erosion in an orogenic wedge. *Nature Geosci.* **1**, 793–799 (2008).
- Whipple, K. X. The influence of climate on the tectonic evolution of mountain belts. *Nature Geosci.* **2**, 97–104 (2009).
- Mercer, J. H. & Sutter, J. F. Late Miocene earliest Pliocene glaciation in southern Argentina—implications for global icesheet history. *Palaeogeogr. Palaeoclimatol. Palaeoecol.* **38**, 185–206 (1982).
- Ramos, V. A. Seismic ridge subduction and topography: foreland deformation in the Patagonian Andes. *Tectonophysics* **399**, 73–86 (2005).

- Tomkin, J. H. Coupling glacial erosion and tectonics at active orogens: a numerical modeling study. *J. Geophys. Res.* **112**, F02015, doi:10.1029/2005JF000332 (2007).
- Porter, S. C. Pleistocene glaciation in the southern Lake District of Chile. *Quat. Res.* **16**, 263–292 (1981).
- Montgomery, D. R., Balco, G. & Willett, S. D. Climate, tectonics, and the morphology of the Andes. *Geology* **29**, 579–582 (2001).
- Egholm, D. L., Nielsen, S. B., Pedersen, V. K. & Leseman, J.-E. Glacial effects limiting mountain height. *Nature* **460**, 884–888 (2009).
- Thomson, S. N. Late Cenozoic geomorphic and tectonic evolution of the Patagonian Andes between latitudes 42°S and 46°S: an appraisal based on fission-track results from the transpressional intra-arc Liqueiñe-Ofqui fault zone. *Geol. Soc. Am. Bull.* **114**, 1159–1173 (2002).
- Brozovic, N., Burbank, D. W. & Meigs, A. J. Climatic limits on landscape development in the northwestern Himalaya. *Science* **276**, 571–574 (1997).
- Broecker, W. S. & Denton, G. H. The role of ocean-atmosphere reorganizations in glacial cycles. *Quat. Sci. Rev.* **9**, 305–341 (1990).
- Willett, S. D. Orogeny and orography: the effects of erosion on the structure of mountain belts. *J. Geophys. Res.* **104**, 28957–28981 (1999).
- Molnar, P. & England, P. Late Cenozoic uplift of mountain ranges and global climate change—chicken or egg? *Nature* **346**, 29–34 (1990).
- Fitzgerald, P. G., Sorkhabi, R. B., Redfield, T. F. & Stump, E. Uplift and denudation of the central Alaska Range: a case study in the use of apatite fission track thermochronology to determine absolute uplift parameters. *J. Geophys. Res.* **100**, 20175–20191 (1995).
- Blisniuk, P. M., Stern, L. A., Chamberlain, C. P., Idleman, B. & Zeitler, P. K. Climatic and ecologic changes during Miocene surface uplift in the southern Patagonian Andes. *Earth Planet. Sci. Lett.* **230**, 125–142 (2005).
- Reiners, P. W., Ehlers, T. A., Mitchell, S. G. & Montgomery, D. R. Coupled spatial variations in precipitation and long-term erosion rates across the Washington Cascades. *Nature* **426**, 645–647 (2003).
- DaSilva, J. L., Anderson, J. B. & Stravers, J. Seismic facies changes along a nearly continuous 24 degrees latitudinal transect: the fjords of Chile and the northern Antarctic peninsula. *Mar. Geol.* **143**, 103–123 (1997).

21. Hervé, F., Pankhurst, R. J., Fanning, C. M., Calderón, M. & Yaxley, G. M. The South Patagonian batholith: 150 my of granite magmatism on a plate margin. *Lithos* **97**, 373–394 (2007).
22. Flynn, J. J. *et al.* A new fossil mammal assemblage from the southern Chilean Andes: implications for geology, geochronology, and tectonics. *J. S. Am. Earth Sci.* **15**, 285–302 (2002).
23. Coutand, I. *et al.* Structure and kinematics of a foothills transect, Lago Viedma, southern Andes (49 degrees 30' S). *J. S. Am. Earth Sci.* **12**, 1–15 (1999).
24. Fosdick, J. C. Late Miocene exhumation of the Magallanes Basin and sub-Andean fold belt, southern Chile: new constraints from apatite U-Th/He thermochronology. *GSA Abstr.* **39**, 341 (2007).
25. Harambour, S. M. Deep-seated thrusts in the frontal part of the Magallanes fold and thrust belt, Ultima Esperanza, Chile. *15th Congr. Geol. Argentino Actas* **3**, 232 (2002).
26. Hulton, N. R. J., Purves, R. S., McCulloch, R. D., Sugden, D. E. & Bentley, M. J. The Last Glacial Maximum and deglaciation in southern South America. *Quat. Sci. Rev.* **21**, 233–241 (2002).
27. Swift, D. A., Persano, C., Stuart, F. M., Gallagher, K. & Whitham, A. A reassessment of the role of ice sheet glaciation in the long-term evolution of the East Greenland fjord region. *Geomorphology* **97**, 109–125 (2008).
28. Sugden, D. E. Glacial erosion by the Laurentide ice sheet. *J. Glaciol.* **20**, 367–391 (1978).
29. Fabel, D. *et al.* Landscape preservation under Fennoscandian ice sheets determined from in situ produced Be-10 and Al-26. *Earth Planet. Sci. Lett.* **201**, 397–406 (2002).
30. Reiners, P. W. & Brandon, M. T. Using thermochronology to understand orogenic erosion. *Annu. Rev. Earth Planet. Sci.* **34**, 19–66 (2006).

**Supplementary information** is linked to the online version of this paper at [www.nature.com/nature](http://www.nature.com/nature).

**Acknowledgements** This work was supported by the NSF Geomorphology and Land Use Dynamics and Tectonics Award EAR0447140. S. Nicolescu assisted with (U–Th)/He analysis. S.N.T. thanks F. Hervé for numerous invitations to take part in boat expeditions in the Chilean fjords made possible through Chilean Fondecyt awards 1010412, 1050431, 7010412 and 7060240. Captains C. Alvarez Senior and Junior, V. Alvarez, D. Lleufo and C. Porter expertly guided us through the Chilean fjords on the boats *Mama Dina*, *Penguin*, *Foam*, *21 de Mayo* and *R/V Gondwana*. We thank R. Fuenzalida and C. Mpodozis at ENAP/Sipetrol for allowing us to publish the apatite fission track data from the SP samples. H. Echterl and J. Glodny at the GFZ Potsdam, and F. Hervé at the Universidad de Chile provided additional apatite sample separates. This work benefited from discussions with G. Roe and M. Kaplan.

**Author Contributions** Writing and interpretation was done by S.N.T. with contributions from M.T.B., J.H.T. and P.W.R. Fieldwork was performed by S.N.T., M.T.B., J.H.T., P.W.R. and C.V. Apatite fission track analysis was done by S.N.T. (U–Th)/He dating was carried out by S.N.T., N.J.W. and C.V.

**Author Information** Reprints and permissions information is available at [www.nature.com/reprints](http://www.nature.com/reprints). The authors declare no competing financial interests. Readers are welcome to comment on the online version of this article at [www.nature.com/nature](http://www.nature.com/nature). Correspondence and requests for materials should be addressed to S.N.T. ([thomson@email.arizona.edu](mailto:thomson@email.arizona.edu)).